J. Membrane Biol. 138, 13–28 (1994)

The Journal of
Membrane
Biology

Association of Acetylcholine Receptors with Peripheral Membrane Proteins: Evidence from Antibody-induced Coaggregation

R.J. Bloch[1], R. Sealock[3], D.W. Pumplin[2], P.W. Luther[1], S.C. Froehner[3]

[1]Department of Physiology, University of Maryland School of Medicine, 660 W. Redwood St., Baltimore, Maryland 21201
[2]Department of Anatomy, University of Maryland School of Medicine, Baltimore, Maryland
[3]Department of Physiology, University of North Carolina School of Medicine, Chapel Hill, North Carolina

Received: 12 July 1993/Revised: 3 November 1993

Abstract. Acetylcholine receptors (AChR) are associated with several peripheral membrane proteins that are concentrated on the cytoplasmic face of the plasma membrane at the neuromuscular junction, and at aggregates of AChR that form in vitro. We tested the linkage among these proteins by inducing microaggregation of AChR, then determining if a given peripheral membrane protein accumulated with the receptors in microaggregates. In most experiments, we used isolated membrane fragments that are rich in AChR and accessible to antibodies against intracellular antigens. We showed that the 43 kD receptor-associated protein always aggregated with AChR, whether microaggregation was driven by antibodies to the 43 kD protein, or to the receptor itself. Antibodies to the 58 kD receptor-associated protein also always aggregated the 58 kD protein with the receptor. Our results are consistent with a model for AChR-rich membrane in which the 43 kD and 58 kD proteins are both closely associated with the AChR.

When we induced microaggregation in intact muscle cells with anti-AChR antibodies, our results were less definitive. The 43 kD receptor-associated protein microaggregated with AChR, but the 58 kD protein was not especially enriched at AChR microaggregates. We discuss the advantages of using isolated AChR-rich membrane fragments to study the association of AChR with peripheral membrane proteins.

Key words: Acetylcholine receptor — Rat myotubes — 43 kD receptor-associated protein — 58 kD receptor-associated protein — Microaggregation — Patching and capping

Correspondence to: R.J. Bloch

Introduction

The nicotinic acetylcholine receptor (AChR) is an integral membrane protein that has been purified and extensively studied (*reviewed in* Changeux, Devillers-Thiéry & Chemouilli, 1984; Stroud & Finer-Moore, 1985). In adult muscle fibers, more than 70% of AChR is concentrated at the neuromuscular junction, which accounts for less than 0.1% of the surface area of the cell. We have been studying the association of AChR with peripheral membrane proteins in Torpedine electric organ and in mammalian muscle to determine how such high local concentrations of AChR develop. We and others have identified a large set of intracellular proteins that are enriched at the neuromuscular junction and that are associated with high concentrations of AChR ("AChR clusters") in cultured muscle cells (Bloch & Pumplin, 1988; Froehner, 1991). Some of these (talin, vinculin, α-actinin, filamin, clathrin) are not directly associated with clustered AChR in vitro, as they can be readily extracted without altering the organization of AChR clusters (Bloch 1984; Pumplin & Bloch, 1990). Others, including actin, β-spectrin, and proteins of M_r 43,000 and 58,000 (here termed 43K and 58K), are more closely associated with AChR. Removal of one or more of these peripheral membrane proteins from AChR clusters is invariably accompanied by severe disorganization of clusters and movement of AChR into regions of the muscle membrane from which they are normally excluded (Bloch, 1986; Bloch & Froehner, 1987; Bloch & Morrow, 1989; Bloch et al., 1991).

Of these proteins, 43K seems most closely associated with AChR-rich membrane, as it remains bound following treatments that remove 58K, β-spectrin and actin (Bloch & Froehner, 1987). Attempts to use reconstitution techniques to demonstrate binding of 43K to AChR have been unsuccessful, however (Porter &

Froehner, 1985). Indirect methods have therefore been used to demonstrate the close association of these two proteins. Several laboratories showed that removal of 43K from AChR-rich membrane, by alkaline pH or by chaotropic agents, alters the properties and mobility of AChR (Rousselet, Cartaud & Changeux, 1979; Lo et al., 1980; Wennogle & Changeux, 1980; Cartaud et al., 1981; Bloch & Froehner, 1987) without inhibiting receptor function (Neubig et al., 1979). Additional evidence for association was obtained from cross-linking experiments, which showed that 43K can be coupled to the β subunit of the AChR (Burden, DePalma & Gottesman, 1983). Most recently, AChR aggregation was observed in *Xenopus* oocytes and fibroblasts that co-express the 43K protein (Froehner et al., 1990; Phillips et al., 1991). Taken together, these results strongly suggest that the 43K protein binds directly to the AChR. Similar experiments have not yet been done to investigate the association of the 58K protein with AChR, however.

We have taken a different approach to study the association of AChR with cytoskeletal or peripheral membrane proteins. We reasoned that, if a protein is tightly bound to AChR, then antibodies that aggregate that protein should also aggregate the AChR. Similarly, antibodies that aggregate the AChR should aggregate the protein. Here, we describe a set of protocols to use with isolated fragments of AChR-rich membrane that confirm a close association between 43K and AChR. We then use these protocols to test the association of AChR with the 58K protein. We report that the 58K protein invariably associates with AChR in antibody-induced microaggregates, suggesting that it, like the 43K protein, is closely associated with clustered AChR. Similar experiments with intact cells confirmed the close association of AChR with 43K but were inconclusive for 58K. Studies of the linkages among AChR and peripheral membrane proteins are therefore more informative with isolated membrane fragments than with intact cells.

Materials and Methods

Culture of Primary Muscle Cells

Primary cultures of rat myotubes were prepared by established procedures (Bloch, 1979; Bloch & Geiger, 1980). Briefly, hind limb muscles from neonatal rats were dissociated in collagenase, and suspended at 10^6 cells/ml in Dulbecco-Vogt modified Eagle's medium containing 10% fetal calf serum (medium). Aliquots of 0.4 ml were applied to glass coverslips (Van Labs, Oxnard, CA), supplemented the next day with 1.5 ml medium, and changed into medium containing 2×10^{-5} M cytosine arabinoside 3 days later. Cells were used on days 6–8 after plating.

Isolation and Extraction of AChR Clusters

AChR clusters were isolated by extraction with saponin, which removes >99% of total cellular protein from cultures, leaving most of the clusters behind on the coverslip (Bloch, 1984). Some cultures were first labeled with monotetramethylrhodamine-α-bungarotoxin (R-BT) (5 μg/ml, in HEPES-buffered DMEM containing 5% fetal calf serum). For extraction with saponin, cells were washed sequentially with phosphate-buffered saline (PBS), and with PBS supplemented with 10 mM $MgCl_2$, 1 mM EGTA, 1 mg/ml bovine serum albumin (BSA). Cultures were then placed in the same solution containing 0.2% saponin, and rocked gently for 4–10 min at room temperature (RT) (Bloch, 1984). Most samples were then placed at 0°C, or treated further and then cooled to 0°C. Samples were maintained at 0°C by keeping them on an aluminum plate in contact with ice.

Some extracted samples were treated before fixation to remove one or more of the peripheral membrane proteins known to be associated with clustered AChR. The treatments and the proteins they are known to extract or degrade are summarized in Table 1. Unless otherwise noted, all treatments are for 5 min at RT. Further details are provided in the references noted in Table 1.

Antibody-driven Microaggregation in Isolated AChR Clusters

After being cooled to 0°C, samples were inverted over a precooled droplet (25–50 μl) of monoclonal antibody diluted in PBS supplemented with 1 mg/ml BSA (PBS-BSA), and incubated for 1 hr. The monoclonal antibodies we used are listed in Table 2. Samples were washed rapidly at 0°C in PBS-BSA, inverted over a droplet of fluorescent anti-antibody at 0°C, and incubated for an additional 60 min. Samples were again washed rapidly at 0°C in PBS-BSA. They were then either placed at RT or maintained at 0°C, for 15 min. All samples were then fixed in 2% paraformaldehyde in PBS, and incubated in 0.1 M glycine in PBS to inactivate remaining aldehydes.

The following steps varied depending on the protocol for double immunofluorescence labeling we followed. In protocol #1, cultures were prelabeled with R-BT before extraction with saponin, and AChR or AChR-associated proteins were labeled with mouse monoclonal antibody (mab) followed by fluoresceinated goat anti-mouse IgG (FGAM). In this case, the fixed samples were simply mounted on slides and observed. In protocol #2, samples were first treated with a mouse mab followed by rhodaminylated rabbit anti-mouse IgG (RRAM). After fixation, samples were incubated in mouse IgG (1 mg/ml) for 15 min, and then exposed to biotinylated mab followed by fluoresceinated avidin (F-Av) or strepavidin (F-SAv). Incubations with biotinylated antibody and F-Av or F-SAv were performed in the presence of 1 mg/ml mouse IgG to block binding of the biotinylated antibody to unoccupied sites on RRAM. After labeling, samples were mounted in nine parts glycerol, one part Tris-HCl, pH 8, supplemented with 1 mg/ml *p*-phenylenediamine, to reduce photobleaching (Johnson et al., 1982).

Treatment of BC3H-1 Cells

BC3H-1 mouse muscle cells (Schubert et al., 1974) were grown for 10–12 days on glass coverslips in medium containing 20% fetal calf serum. They were incubated for 45 min at 37°C with 130 nM R-BT and rabbit anti-AChR serum (1:100) which reacts with extracellular epitopes of the AChR (Froehner, 1981). The incubation was continued for the indicated time at 37°C, and the cells were rinsed briefly two times with culture medium. Cultures were then incubated with sheep anti-rabbit IgG (1:400 dilution) for the indicated times at 37°C, rinsed three times with medium, fixed with 1% paraformaldehyde, 100 mM lysine, 0.1% saponin, pH 7.3, for 20 min at RT and rinsed with PBS. All subsequent incubations were done at RT. The fixed cells were treated sequentially with PBS/1% Triton X-100 for 10 min to permeabilize the cells, with PBS/$NaBH_4$ (1 mg/ml) for 30 min, and with PBS/4% BSA/10% calf serum (buffer used for antibody incu-

Table 1. Removal of proteins from isolated AChR clusters

Protein	Extraction procedure				Reference
	Buffer A[a]	PBS[b]	CT[c]	pH 11[d]	
Actin	Removed	—[e]	Removed	Removed[f]	(Bloch, 1986, *and unpublished*)
β-Spectrin	Bound	Removed[g]	Removed	Removed	(Bloch & Morrow, 1989)
Dystrophin[h]	Bound	Bound	Removed	Bound	(Dmytrenko, Pumplin & Bloch, 1992)
58K	Bound	Bound	Removed	Removed[f]	(Bloch et al., 1991)
43K	Bound	Bound	Bound	Removed	(Bloch & Froehner, 1987)
AChR	Bound	Bound	Bound	Bound	(Bloch & Froehner, 1987)

[a] 1 mM Tris HCl, 0.1 mM ATP, pH 8.0, for 10 min at RT.
[b] 10 mM NaP, 145 mM NaCl, pH 7.2. Similar results are obtained at 5 or 10 min at RT.
[c] 10 μg/ml chymotrypsin in PBS at RT.
[d] 50 mM ethanolamine-HCl, pH 11, 5 min, RT.
[e] Not determined.
[f] Removal is partial, not complete.
[g] Removal is by slow dissociation, with a $t_{1/2}$ of ~20 min (Bloch & Morrow, 1989).
[h] Dystrophin is only a minor component of AChR clusters (Dmytrenko et al., 1992).

Table 2. Monoclonal antibodies used

Antibody	Species	Specificity	Reference
88B	Mouse	AChR γ and δ chains	(Froehner et al., 1983)
1234A	Mouse	43K	(Froehner, 1984)
1579A	Mouse	43K	(S.C. Froehner, *unpublished*)
1351E	Mouse	58K	(Froehner et al., 1987)

bations) for 30 min. The cultures were then incubated overnight with a mixture of two anti-43K mabs (mab 1234 and 1579, 20 nM IgG each) that recognize distinct epitopes (Froehner, 1984; S.C. Froehner, *unpublished*), or a control mab IgG (40 nM). Cultures were rinsed with PBS and incubated sequentially for 90 min with FGAM and fluoresceinated sheep anti-goat IgG (FSAG), each diluted 1:1000 in antibody buffer.

In some experiments, cultures were treated as described above but anti-58K mab 1351 was substituted for the anti-43K mabs. To examine the association of 43K with other antibody-induced clusters of membrane antigens, live BC3H-1 cells were incubated sequentially with rabbit anti-mouse lymphocyte serum (1:50 dilution; Microbiological Associates) and with rhodaminylated sheep anti-rabbit IgG for 45 min each. Cultures were then fixed and labeled with anti-43K mabs, as described above.

Microscopy and Photomicrography

Samples were observed with a Zeiss IM-35 (isolated AChR clusters) or Universal (BC3H-1 cells) microscope equipped for epifluorescence. Photomicrographs were exposed for 15–30 sec. Ilford HP5 film was processed with Ilford Microphen developer (Ilford, Basildon, Essex, UK) to an ASA of 1,600.

Analysis of Microaggregation by Digital Imaging

Some control and microaggregated samples were observed with a Zeiss Planapo 63X/NA 1.4 objective on a Zeiss upright fluorescence microscope equipped with a slow scan charge-coupled device camera (CH250 with Kodak KAF-1400 CCD, Photometrics, Tucson, AZ). Images were displayed and analyzed on a dedicated MacIIci computer (Apple Computer, Cupertino, CA) running the NIH Image program. Each pixel represented a 0.01 μm^2 portion of the image. Digitized images were photographed on 35 mm film with a film recorder (Montage FR1, Presentation Technologies, Sunnyvale, CA).

Sequential Observations

AChR clusters labeled with R-BT were isolated with saponin, extracted at pH 11 and exposed to 88B anti-AChR mab, as described above. The specimens were mounted in a precooled perfusion chamber filled with PBS-BSA, and maintained at 0°C with ice placed on the back of the chamber. Fluorescence observations were made through a Leitz Planapochromat 63X/NA 1.4 objective. Photodynamic damage (Olek, Pudimat & Daniels, 1983) was minimized by reducing the excitatory light from the mercury arc 10-fold with a neutral density filter, and by using a filter set configured for low light level fluorescence of tetramethylrhodamine (excitation: 546 DF10; dichroic: 560 DRLP; emission: 560 EFLP; Omega Optical, Brattleboro, VT). Images of areas that had diffuse R-BT labeling were collected with a slow-scan, charge-coupled device camera (Star 1, Photometrics, Tucson, AZ; integration time, 10 sec). Once a set of images was collected, FGAM was introduced into the perfusion chamber. After 15 min, the chamber was warmed to RT for 15 min. Stage coordinates were used to return to the location of each original image, and a second set of images was collected.

Freeze-Fracture Electron Microscopy

After exposure to antibodies, samples were fixed in 2% paraformaldehyde followed by 2% glutaraldehyde in 0.1 M phosphate buffer, then freeze-fractured by the complementary replica method using polyvinyl alcohol (Pauli et al., 1977), previously described (Pumplin & Bloch, 1983). Circles (4 mm diameter) were cut from the coverslips in areas containing many myotubes. Samples were cryoprotected by exposure to 33% (vol/vol) glycerol for 30 min, sandwiched with a drop of polyvinyl alcohol solution (25% in 33% glycerol) and a specimen carrier, then frozen in barely melted Freon 22. They were freeze-fractured at −119°C and $<10^{-6}$ torr and replicated with platinum applied at 45°C followed by a backing film of carbon applied at 90°C. Replicas from the specimen carrier were floated on water and picked up

on Formvar-coated slot grids for examination. These replicas contain the cytoplasmic leaflets (P faces) of plasma membrane in which AChR clusters are found. Replicated clusters were identified as IMP-rich areas of membranes having the characteristic elongated shape of myotubes. A representative area from each cluster was photographed at 20,000×. To avoid possible bias, the microscopist did not know the treatment protocol followed for each grid being examined.

Materials

Mouse IgG and all fluorescent reagents were obtained from Jackson Immunoresearch (West Chester, PA). Secondary antibodies were species-specific. Biotinylation of mabs and of mopc 21 IgG was as described (LaRochelle & Froehner, 1986). Unless otherwise noted, all other materials were purchased from Sigma Chemical (St. Louis, MO).

Results

Our aim in these experiments was to determine whether microaggregation of AChR by antibody-induced crosslinking would cause microaggregation of receptor-associated proteins, and *vice versa*. We first established the validity of this approach by studying AChR and 43K in isolated fragments of myotube membrane rich in AChR, and then extended our observations to the relationship between AChR and 58K in these same preparations. A final series of experiments examined whether a similar approach could be used in intact muscle cells.

Isolated AChR Clusters

AChR clusters of cultured rat myotubes form preferentially where the myotube attaches to the substrate (Land et al., 1977; Bloch & Geiger, 1980; Axelrod, 1981). Upon extraction of myotube cultures with saponin, >99% of the cellular protein is lost, but clusters remain attached to the coverslip, and they maintain their original organization (Bloch, 1984). AChR in freshly isolated clusters are immobile; selective removal of one or more of the receptor-associated proteins renders them more mobile (R. Bloch and M. Edidin, *unpublished results*), and capable of moving into nearby membrane regions (Bloch, 1986; Bloch & Froehner, 1987; Bloch & Morrow, 1989). A list of the treatments that mobilize AChR, and of the proteins known to be removed from clusters by these treatments, is given in Table 1.

AChR

We assessed our microaggregation procedures (*see* Materials and Methods) by using R-BT as a marker for AChR, and a mouse anti-AChR mab (88B) and FGAM to induce microaggregation. Preparations of isolated clusters were extracted at alkaline pH, to remove all major peripheral proteins from the cytoplasmic face of the membrane (Table 1), without removing bound R-BT (Bloch & Froehner, 1987); they were cooled to 0°C, and incubated with 88B followed by FGAM. After washing at 0°C, one sample was warmed to RT for 15 min while another was maintained on ice for the same period. Both were then fixed in paraformaldehyde. Almost all of the receptor-rich membrane fragments kept at 0°C retained the almost uniform distribution of label (Fig. 1*C,D; see also* Figs. 6–8) typical of alkaline-extracted samples (Bloch & Froehner, 1987), whereas most of the fragments warmed to RT appeared punctate and showed distinct dark regions poor in AChR (Fig. 1*A,B; see also* Figs. 6–8). As expected, the microaggregates were also labeled by 88B and FGAM (*cf.* arrowheads in Fig. 1*A,B*). This was confirmed by analysis of digitized images (*see below*). These results suggest that AChR microaggregates form when alkaline-extracted clusters are treated with antibodies and then warmed to RT.

Microaggregation presumably requires cross-linking of AChR and movement of AChR within the plane of the membrane. We did several experiments to test these requirements. (i) Samples that were incubated in 88B but not in FGAM, or in FGAM but not in 88B, did not undergo significant microaggregation upon warming to RT (*not shown*). Thus, neither antibody alone, nor warming samples to RT, is sufficient to induce microaggregation. (ii) Samples incubated with 88B and FGAM but fixed in paraformaldehyde before warming did not undergo microaggregation. (iii) Microaggregation is slowed but not completely blocked at 0°C. If incubation at 0°C is extended for 2–4 hr, samples showed significant microaggregation. These results suggest that receptors must be crosslinked by 88B and FGAM and must be relatively free to diffuse in the membrane for microaggregation to occur.

We studied the microaggregation process further to determine its time course. Complete microaggregation could be observed in samples incubated with each antibody for only 15 min at 0°C, followed by warming to RT for only 5 min. The time course of appearance of microaggregates upon warming was quite rapid, with a half-time of about 90 sec (Fig. 2). Although we used these shorter incubations in some of the experiments described here, we usually incubated our samples for 1 hr with each antibody, and then warmed them for 15 min.

The simplest interpretation of our data is that bivalent antibodies bind to AChR in muscle membrane fragments, and, when the AChR-antibody complex is free to diffuse, crosslink them into microaggregates. We considered two alternative explanations. First, because we compared populations of AChR-rich membrane fragments, we may have only selected those that supported our expectations of microaggregation. This was unlikely, as double blind comparisons of pairs of samples incubated at 0°C and at RT invariably identified the 0°C sample as having fewer microaggregates

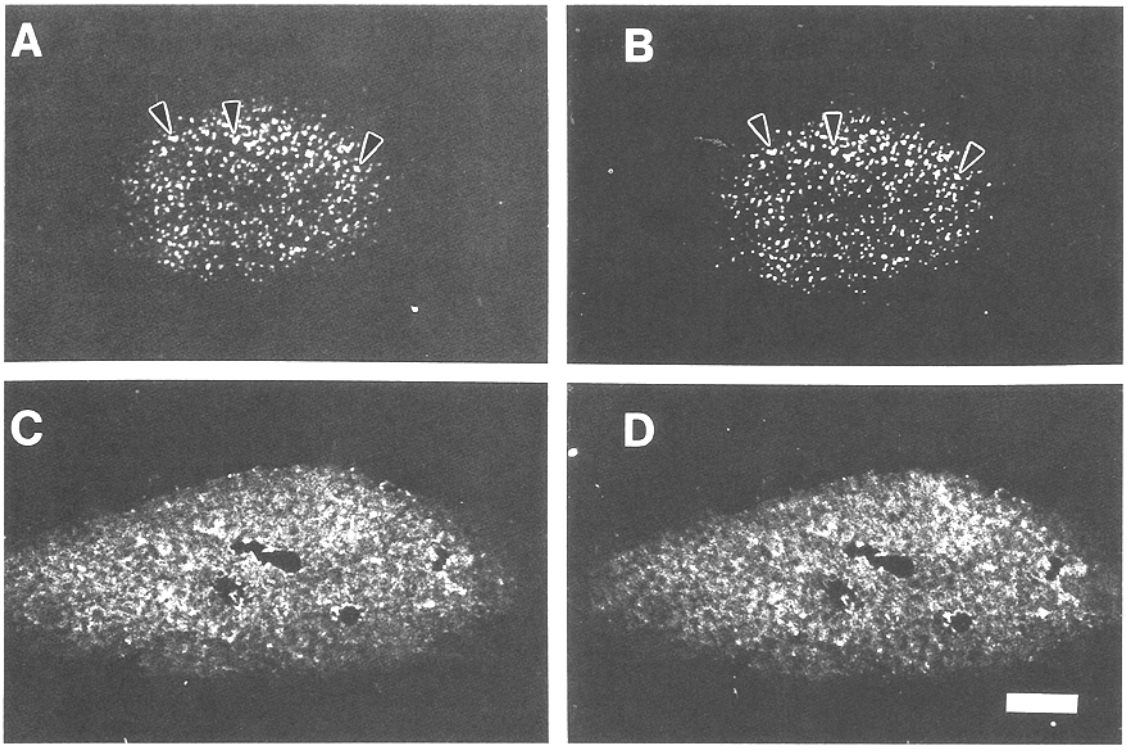

Fig. 1. Microaggregation of AChR induced by anti-AChR antibodies. Cultures of rat myotubes were labeled with R-BT, and AChR clusters were isolated by extraction with saponin. Isolated clusters were extracted further at alkaline pH and cooled to 0°C. Samples were incubated for 1 hr each with 20 nM 88B anti-AChR and FGAM. After washing at 0°C, samples were incubated for 15 min in buffered saline at RT (*A,B*) or at 0°C (*C,D*). *A* and *C* show 20 nM 88 B R-BT label; *B* and *D* show labeling by antibodies. (*A,B*) Sample incubated at RT shows microaggregates that label with R-BT (*A*, arrowheads) and with antibodies (*B*, arrowheads); (*C,D*) sample incubated at 0°C shows much less microaggregation, with more uniform labeling by both R-BT (*C*) and antibodies (*D*). Scale bar = 10 μm.

than the RT sample. (Similar double blind studies on freeze-fractured membranes (*see below*) also made this selection hypothesis unlikely). We tested this possibility further by following the redistribution of AChR in individual membrane fragments immediately after samples were brought to RT. We avoided full fluorescence illumination of the samples, as this prevented antibody-induced microaggregation (*see* Materials and Methods). Because of the rapid time course of microaggregation (Fig. 2), the sample was warmed to RT only after it was mounted on the microscope. Under these conditions, AChR that were almost uniformly distributed at 0°C (Fig. 3*C*) formed microaggregates within a short time after warming (Fig. 3*D*). If incubation with 88B was omitted, microaggregation did not occur (Fig. 3*A,B*). Thus, microaggregation can be observed on individual membrane fragments and cannot be explained by observer bias.

Another explanation of our results is that warming of antibody-labeled membranes destabilizes the lipid bilayer, resulting in finely disrupted membrane that appears to contain microaggregates of AChR. Isolated clusters treated with the chaotropic agent, lithium diiodosalicylate, may undergo such a transition (Bloch & Froehner, 1987). We examined this possibility in two different ways. (i) We labeled microaggregated samples with a fluorescent probe (C_{18}-diI) that partitions preferentially into the lipid bilayer. We saw no evidence that regions of the membrane in microaggregated samples were disrupted (Scher & Bloch, 1991). (ii) We extracted AChR clusters at alkaline pH, treated them with 88B and FGAM and, after maintaining them at 0°C or warming them to RT, we fixed the samples and subjected them to freeze-fracture electron microscopy (Fig. 4). Freeze-fracture cleaves the bilayer between the two lipid leaflets, and tears in the membrane are readily observable with this technique. Membranes appeared intact in samples treated at RT (Fig. 4*C*), in samples kept at 0°C (Fig. 4*A*), or in samples warmed to RT but not previously exposed to antibodies (Fig. 4*B*). Samples labeled with antibodies and warmed to RT showed large aggregates of large, angular intramembrane particles (IMP: Fig. 4*C*), known to correlate with AChR (Yee, Fischbach & Karnovsky, 1978; Cohen & Pumplin, 1979; Heuser & Salpeter, 1979), consistent with the light microscopic observations shown above. Such aggregates were uncommon in two control samples (Table 3). Double blind sorting of photomicrographs reliably distinguished images of samples incubated at RT from those kept at 0°C or those not exposed to antibodies (*P*

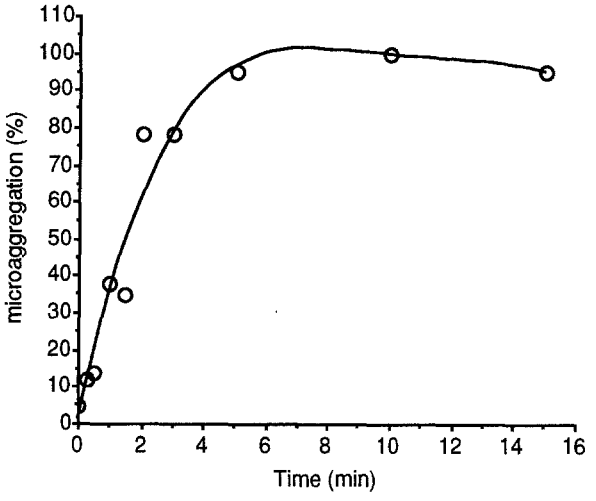

Fig. 2. Time course of microaggregation upon warming to RT. Samples were labeled with R-BT, extracted with saponin and then with 50 mM ethanolamine, pH 11, cooled to 0°C, and incubated with 25 nM 88B anti-AChR mab for 15 min. Samples were washed at 0°C, and incubated for an additional 15 min at 0°C with FGAM. After washing at 0°C, samples were placed into PBS at RT and then fixed in paraformaldehyde at different times thereafter. Samples were scored for the predominance of microaggregates in each isolated membrane fragment. At least 50 fragments were counted for each point. The results show that microaggregation is essentially complete within 5 min of warming.

< 0.0001, Rank sum test). Thus, our ultrastructural studies support the idea that anti-AChR antibodies and secondary antibodies induce the redistribution of AChR in muscle membrane without causing significant damage to the lipid bilayer.

These experiments show that microaggregation of AChR induced in isolated fragments of muscle membrane is the result of antibody-induced crosslinking and redistribution of AChR within the plane of the muscle membrane. We use this approach to assess the relationship between AChR and proteins believed to be closely associated with it.

43K

To assess the relationship between AChR and 43K, we labeled AChR with R-BT, isolated them by extraction with saponin, and treated them with chymotrypsin. This treatment removes all major proteins but 43K from the cytoplasmic face of cluster membrane (Table 1). We incubated these samples at 0°C with anti-43K mabs and FGAM, warmed some to RT, and then fixed with paraformaldehyde (protocol #1: *see* Materials and Methods). Samples incubated at RT showed microaggregates that labeled both with R-BT and with antibodies (Fig. 5*A,B*, arrowheads), whereas samples incubated at 0°C showed little evidence of microaggregation of either label (Fig. 5*C,D*). Both anti-43K mab and FGAM were necessary for microaggregation, and microaggregation was blocked by prefixation (*not shown*). We conclude that moving 43K into microaggregates with anti-43K mabs and FGAM induces coaggregation of AChR.

We devised a different procedure to determine if aggregating AChR with anti-AChR mabs and FGAM induced coaggregation of 43K (protocol #2: *see* Materials and Methods). As in our earlier experiments, we used 88B and fluorescent GAM (in this case RGAM) to microaggregate AChR, but we did not prelabel AChR with R-BT. After warming samples to RT, we probed for 43K with biotinylated anti-43K mab and fluoresceinated avidin (F-Av) or streptavidin (F-SAv). We found that 43K coaggregated with AChR in samples incubated at RT (Fig. 5*E,F*) but not at 0°C (Fig. 5*G,H*). We used biotinylated control mouse mopc 21 mab to determine if biotinylated anti-43K mab labeled microaggregates nonspecifically, e.g., by binding to unoccupied binding sites on RGAM. Such controls showed no nonspecific binding (*not shown*), suggesting that the precautions taken to block nonspecific binding sites with mouse IgG were adequate (*see* protocol #2, Materials and Methods). Labeling by biotinylated anti-43K mab was also eliminated in samples that were first extracted at alkaline pH, which removes the 43K protein.

Thus, whether microaggregation is driven by antibodies to AChR or by antibodies to 43K, these two proteins redistribute together. This suggests that 43K and AChR are bound (directly or indirectly) to one another.

58K

The M_r 58,000 protein (58K) codistributes with AChR in isolated clusters, but it is also found in other regions of muscle cells (Froehner et al., 1987; Bloch et al., 1991). We used protocol #1 to study its association with AChR. We labeled AChR clusters with R-BT, isolated them by extraction with saponin, and treated them at low ionic strength, which redistributes AChR in the membrane fragments but leaves 58K bound (Table 1) (Bloch et al., 1991). Samples were cooled to 0°C, incubated with an anti-58K mab (1351E: *see* Table 2) and FGAM, washed, and incubated further at 0°C or RT before fixation. Unlike previous samples, samples were analyzed in digital images (Fig. 6) obtained with a CCD camera interfaced with a Macintosh computer (*see* Materials and Methods). As controls for this method of analysis, we also processed samples treated with antibodies to AChR. All samples warmed to RT showed coaggregation of R-BT and the antibody labels, but little or no microaggregation was seen in samples maintained at 0°C (Fig. 6). Microaggregates were not as clearly visible in these samples as they were in earlier experiments, however.

We evaluated the differences between samples quantitatively on digitized images in two ways, one to determine if the differences in distribution of R-BT flu-

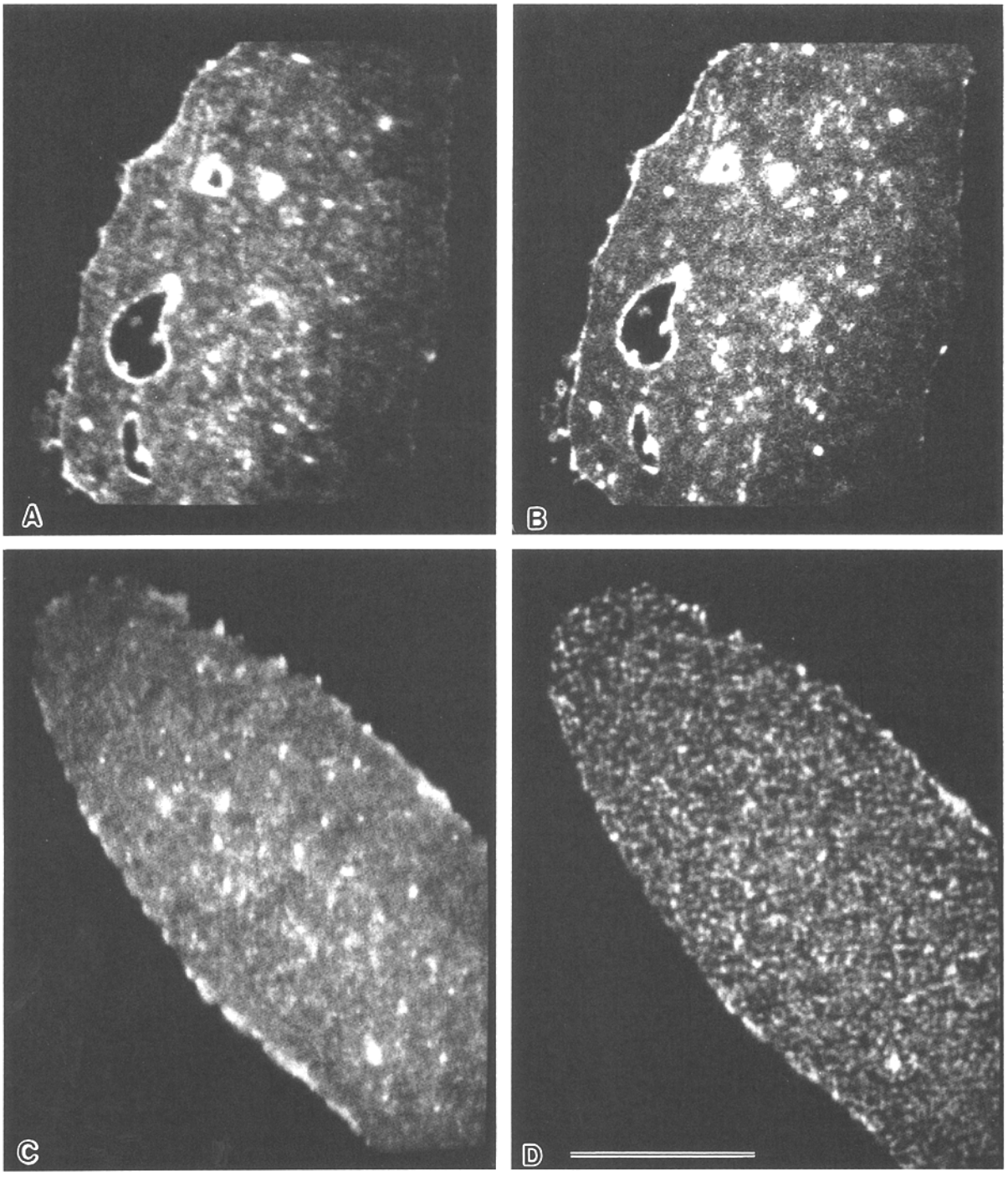

Fig. 3. Sequential observations of microaggregation on identified clusters. Samples were labeled with R-BT, extracted with saponin and with 50 mM ethanolamine, pH 11, and cooled to 0°C. Samples were incubated in the absence (*A,B*) or presence (*C,D*) of 88B anti-AChR for 15 min at 0°C, transferred to a perfusion chamber on ice, and placed on the microscope stage. The sample was kept cold by placing ice on the upper surface of the perfusion chamber. After images were collected under reduced fluorescence illumination at 0°C (*A,C*), FGAM was added to the chilled chamber and the sample was allowed to reach RT. After 20 min, a second rhodamine image of the same cluster was collected. (*B,D*). (*A,B*) Sample incubated without 88B but with FGAM. The almost uniform labeling by R-BT seen at 0°C (*A*) does not change upon warming (*B*). (*C,D*) Sample incubated with both 88B and FGAM. The almost uniform labeling pattern seen at 0°C (*C*) becomes microaggregated upon warming (*D*).

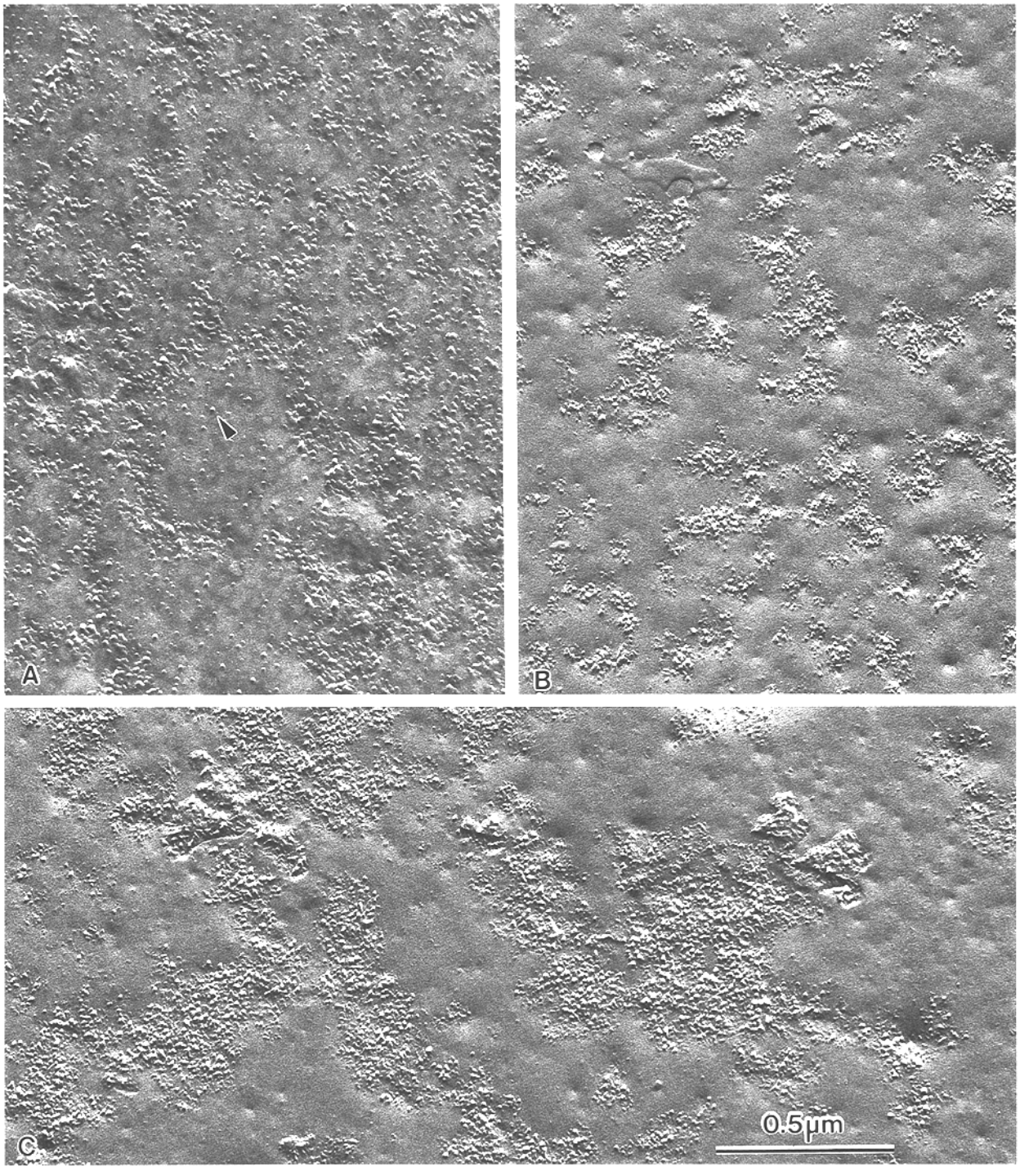

Fig. 4. Freeze-fracture electron microscopy of microaggregates and controls. Three cultures of rat myotubes were labeled with R-BT. AChR clusters were isolated by extraction with saponin, then further extracted at pH 11. Two culture dishes were labeled with 88B anti-AChR antibody followed by FGAM; one of these cultures was incubated 15 min at RT to allow microaggregation, while the other was kept at 0°C for the same time. A third dish was incubated only with FGAM and kept at RT for 15 min. All cultures were then fixed and freeze-fractured by the complementary replica technique (*see* Materials and Methods). AChR clusters were identified in replicas by a relatively high concentration of intramembrane particles (IMP) in a widened area of ventral membrane characteristic of myotubes, and one such area from each cluster was photographed for further analysis (Table 3). IMP in these areas were classified as nonaggregated (*A;* one IMP indicated by the arrowhead), forming small aggregates (*B*), or forming large aggregates (*C*). Small aggregates or nonaggregated IMP predominated in antibody-treated myotubes kept at 0°C (*A*) and in myotubes that were brought to RT without exposure to the primary antibody (*B*). Large aggregates predominated in antibody-treated myotubes incubated at RT (*C*).

Table 3. Analysis of microaggregation by freeze-fracture electron microscopy

Treatment	Aggregation of IMP[a]		
	Large	Small	None
No primary Ab[b]	2	13	17
88B, 0°C[b]	4	20	9
88B, RT[c]	19	12	0

For analysis, one electron micrograph was taken from each cluster observed on a grid. To avoid possible bias, the microscopist did not know the treatment protocol of the grid being examined. A total of 31–33 micrographs from each treatment (96 micrographs in all) were coded and presented in random order to an experienced observer who rated the degree of aggregation of IMP in each (*cf.* Fig. 3). The results were analyzed by Chi^2 tests of the appropriate 2×3 contingency tables. Independent ratings by two other observers agreed closely. [a]Number of micrographs in which IMP had the indicated degree of microaggregation. [b]Treatments not significantly different ($P = 0.1$). [c]Treatment significantly different from others ($P = 0.0001$).

orescence were significant, the other to determine if fluorescence of R-BT and of the secondary antibody were coincident. For the first analysis, we reasoned that if AChR were well dispersed after extraction of peripheral proteins, then an approximately equal amount of R-BT should appear in each pixel area, and therefore all pixels should have approximately the average (intermediate) gray level. Conversely, microaggregation of AChR should be reflected in an increased number of pixel areas having either more AChR (giving an increased R-BT fluorescence) or less AChR (giving a decreased fluorescence) than the average. Equal-sized areas (125–200 × 50–70 pixels) were taken from the R-BT images of samples incubated at 0°C or RT. A histogram of the percentage of total pixels having each gray level was computed for each image (Fig. 7). In samples held at RT, the percentage of pixels having high and low levels of fluorescence increased at the expense of pixels having intermediate levels of fluorescence, consistent with microaggregation. The differences in the shapes of the histograms for each antibody were significant ($P < 0.01$), as shown by applying the Kolmogorov test to the cumulative forms of the histograms.

We next analyzed the relationship between the levels of fluorescence intensity for the R-BT and FGAM images of the same membrane area. If microaggregation of AChR is due to antibody crosslinking of a protein attached to the AChR, pixels with high R-BT fluorescence should also be high in antibody fluorescence, and *vice versa.* To test this, we examined gray levels along bands three pixels wide taken across the entire width of the image. By referring to distinctive features, we were able to select identical areas from the fluorescein and rhodamine images. The intensities of rhodamine and fluorescein fluorescence in these bands were highly correlated (Fig. 8), with values of r ranging from 0.71 to 0.88 ($P < 0.0001$ in all cases). Comparisons of fluorescence from two bands in different regions of the same cluster or from different clusters were not correlated ($r < 0.1$, $P > 0.1$). These findings show that treatment of AChR or 58K with antibodies under conditions allowing lateral diffusion induces changes in the distribution of R-BT fluorescence. Furthermore, they show that the distribution of 58K is closely correlated with that of AChR, regardless of the degree of microaggregation.

Intact Cells

Having established that microaggregation of AChR in isolated AChR-rich membrane fragments could be used to establish a close correlation between AChR and the 43K and 58K proteins, we performed similar studies on intact cells. The BC3H-1 cell line is a nonfusing, mouse muscle cell that produces high concentrations of surface AChR (Schubert et al., 1974) and approximately equivalent amounts of 43K (LaRochelle & Froehner, 1986). BC3H-1 cells do not normally form AChR clusters and show only uniform staining of low intensity after labeling with R-BT or after fixation, permeabilization and labeling with anti-43K mabs. This suggests that there are few endogenous sites in BC3H-1 cells where AChR or 43K are concentrated.

Incubation of R-BT-labeled BC3H-1 cells with anti-AChR antibodies directed against extracellular determinants of the AChR followed by incubation with sheep anti-rabbit IgG, caused the formation of small, strongly fluorescent aggregates (Fig. 9*A*). These microaggregates presumably arose by coalescence of mobile, diffusely distributed AChR, as do microaggregates induced by biotinylated α-bungarotoxin and avidin (Axelrod, 1980). When these samples were fixed, permeabilized and labeled with anti-43K mabs, followed by FGAM and FSAG, there was a striking coincidence of microaggregates labeled with both rhodamine and fluorescein (e.g., arrowheads in Fig. 9*A,B*). Neither AChR clusters nor punctate fluorescein staining was visible in cells treated with control rabbit serum in place of anti-AChR (*not shown*) or when control mouse IgG was substituted for anti-43K mabs (Fig. 9*C,D*). Control experiments showed that the secondary antibodies we used were species-specific. We conclude that AChR microaggregates induced by external application of anti-AChR antibodies contain the muscle homologue of 43K.

43K did not associate with other aggregates of muscle membrane proteins. We induced microaggregates of muscle membrane antigens by sequentially incubating BC3H-1 cells with rabbit anti-mouse lymphocyte serum and rhodaminylated sheep anti-rabbit IgG (Fig. 9*E*). These intensely fluorescent structures were not stained by either anti-43K mabs (Fig. 9*F*) or by anti-AChR mab (*not shown*). Thus, the association of 43K with an-

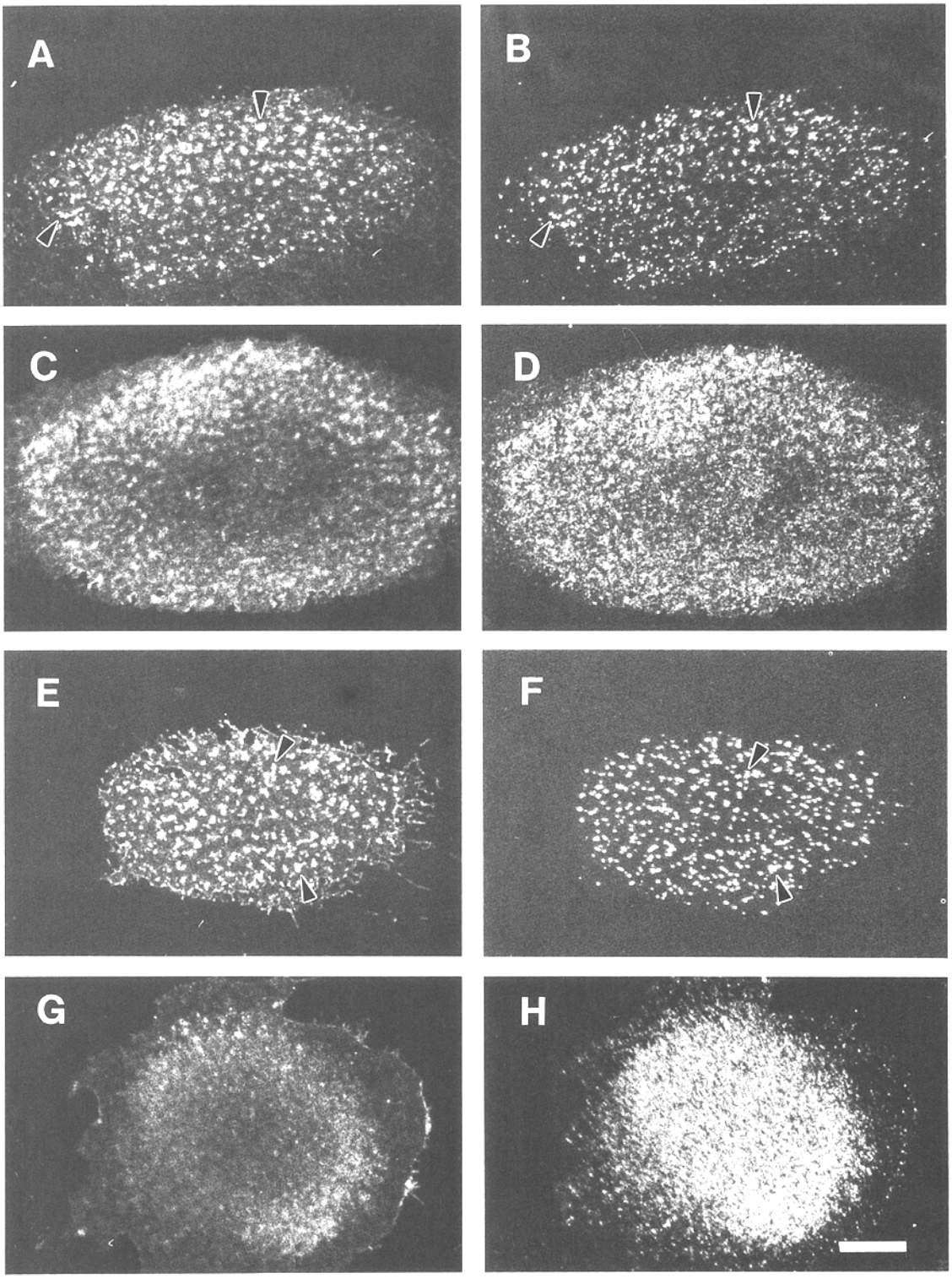

Fig. 5. Coaggregation of AChR and 43K. (*A–D*) Coaggregation induced by antibodies to 43K. Rat myotube cultures were labeled with R-BT and extracted with saponin to isolate AChR clusters. Isolated clusters were treated with chymotrypsin, washed in buffered saline and cooled to 0°C. Samples were incubated with 100 nM each of anti-43K mabs 1234A and 1579A, followed by FGAM. *A* and *C* show labeling by R-BT; *B* and *D* show labeling by antibody. (*A,B*) Sample, warmed to RT after incubation with antibodies, shows microaggregates that are labeled by R-BT (*A,* arrowheads) and antibodies (*B,* arrowheads); (*C,D*) Sample kept at 0°C shows little microaggregation of either label. (*E–H*) Coaggregation induced by antibodies to AChR. Clusters were isolated and treated with chymotrypsin, as above, but were not prelabeled with R-BT. Samples were cooled to 0°C and incubated with 20 nM 88B anti-AChR followed by RGAM. Some were kept further at 0°C; others were warmed to RT. After fixation, all samples were stained further with biotinylated 1579A anti-43K and F-Av (Protocol #2: *see* Materials and Methods). *E* and *G* show labeling of AChR; *F* and *H* show labeling of 43K. (*E,F*) Sample, warmed to RT, shows microaggregates that label for both AChR and 43K; (*G,H*) Sample kept at 0°C shows almost uniform distribution of both labels. Bar = 10 μm.

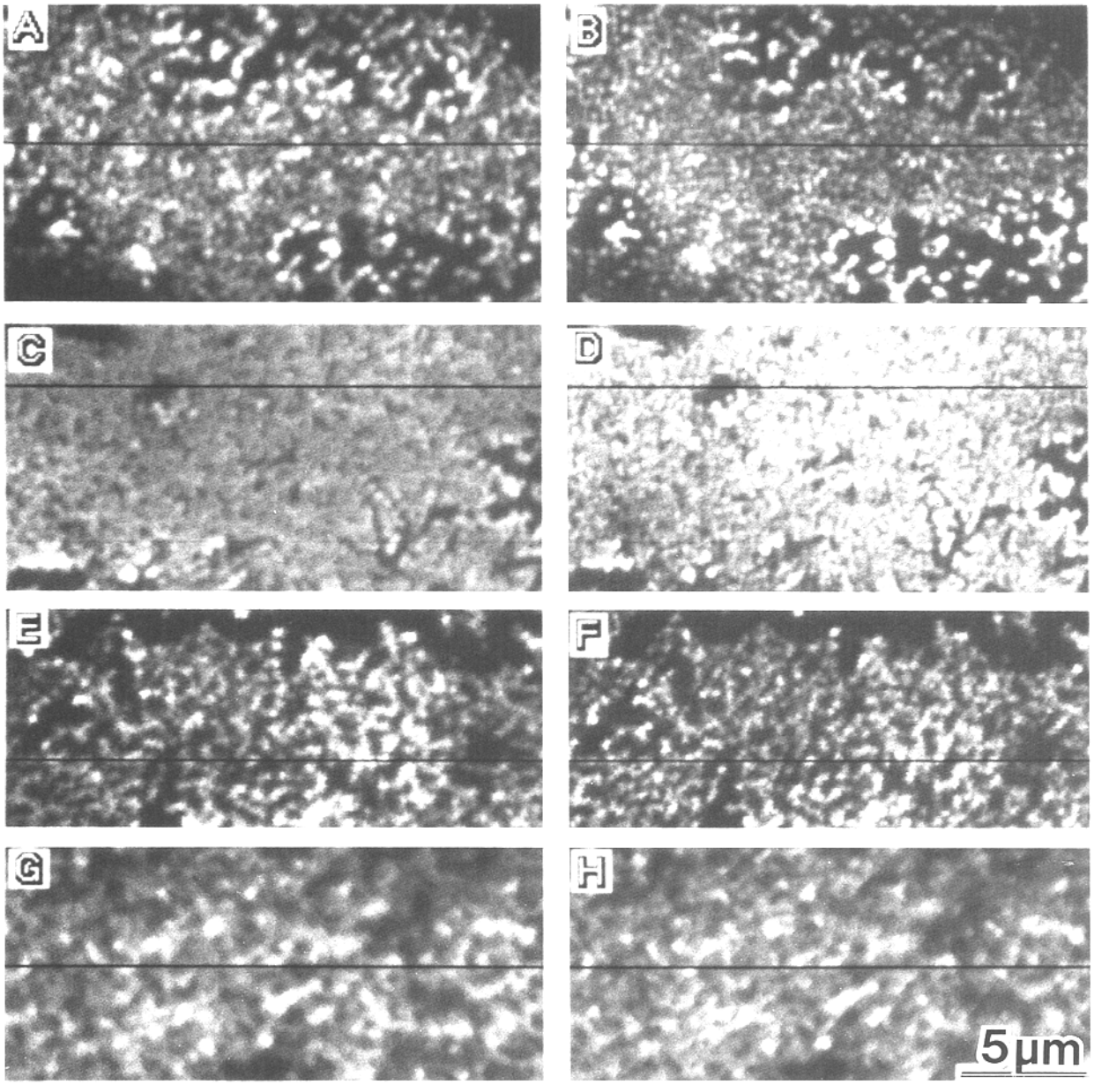

Fig. 6. Coaggregation of AChR and 58K. Samples were labeled with R-BT, extracted with saponin and at low ionic strength, cooled to 0°C, and labeled with 100 nM anti-58K mab 1351 or 20 nM anti-AChR mab 88B, followed by FGAM. After incubation with antibodies, the samples were held at 0°C (*C,D,G* and *H*) or were warmed to RT for 15 min (*A,B,E* and *F*) prior to fixation. With the program, NIH Image, the panels were cut from digitized images obtained with a CCD camera, superimposed by reference to features in the images, and cropped so that when the borders coincided, the corresponding areas of the images were also superimposed to within one pixel. These digitized images were printed from 35 mm negatives made on a high resolution film recorder. Samples incubated in the cold have relatively even distributions of fluorescein and rhodamine fluorescence across the membrane area, while warmed samples have an uneven distribution appearing as a mosaic of light and dark regions. Membrane areas in the panels were analyzed further (*see text* and Figs. 7 and 8). Dark lines indicate the positions of bands analyzed for correlations between fluorescein and rhodamine fluorescence. (*A,B*) Labeled with R-BT (*B*), then with anti-58K antibody and FGAM (*A*), and warmed to RT. (*C,D*) Labeled with R-BT (*D*) and anti-58K antibody and FGAM (*C*), but kept at 0°C. (*E,F*) Labeled with R-BT (*F*) and anti-AChR antibody and FGAM (*E*), and warmed to RT; (*G,H*) Labeled with R-BT (*H*) and anti-AChR antibody and FGAM (*G*), but kept at 0°C. The scale bar in H applies to all panels.

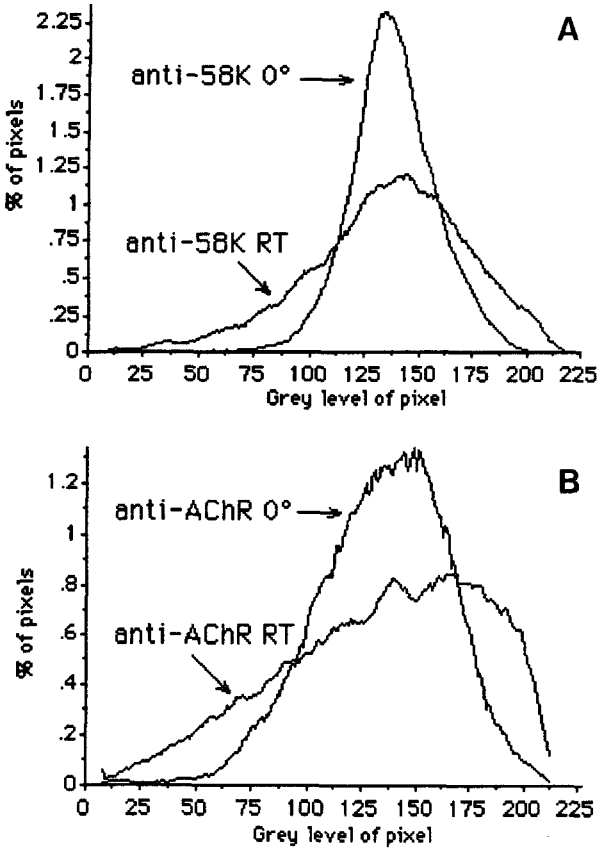

Fig. 7. Histogram of grey levels in control and microaggregated samples. The distribution of fluorescence among pixels is altered in the direction of microaggregation in samples incubated with antibody at RT. This is reflected as a change in the histogram showing the percentage of pixels having each gray level. Portions (125 × 70 pixels) of the rhodamine images shown in Fig. 6 that contained only membrane were used to compute these histograms. To make the average gray level of the two images equal, the difference between the average gray levels of the two images was added to the gray level of each pixel in the lighter image. This correction was less than 10% and did not change the shape of the histogram. For clarity in presentation, the lines were smoothed by applying a 9-point smoothing average; this did not affect the overall shape of the curves or the statistical analysis. The histogram of samples incubated at 0°C is more sharply peaked in all cases, indicating a higher percentage of pixels with intermediate levels of fluorescence. This is consistent with a relatively even distribution of fluorophores in the original image. In samples incubated at RT, the histogram is flattened and spread out, indicating that the image contains more pixels with high and low amounts of fluorescence and fewer pixels with intermediate levels. This is consistent with microaggregation of fluorophores into some pixels and removal of fluorophores from others. Differences between the curves were significant in all cases ($P < 0.01$), as shown by applying the Kolmogorov test to the cumulative forms of the histograms.

tibody-induced microaggregates of AChR appears to be specific.

When we used the same approach to study the association of 58K with AChR, we could detect no apparent enrichment of 58K with microaggregates of AChR (Fig. 9*G,H*). Labeling for 58K in control cells was considerably brighter than labeling for 43K, suggesting that, as in other muscle cells (Froehner et al., 1987), much of the 58K protein in BC3H-1 cells is not associated with AChR. This higher but specific background signal made it difficult to determine if some 58K did coaggregate with AChR.

Discussion

We have established a set of microaggregation protocols to assess the linkage between AChR and AChR-associated proteins in mammalian muscle cells in vitro. Using these protocols, we show that the AChR is as likely to be associated with the 58K protein as it is with the 43K protein.

Some of our experiments resemble "patching and capping" experiments carried out on lymphocytes and other mononucleate cells, in which redistribution of a surface antigen, driven by binding of antibodies against extracellular determinants, is accompanied by corresponding redistribution of intracellular proteins (Taylor et al., 1971; Raff & De Petris, 1973). Our results with intact BC3H-1 cells suggest that 43K and AChR coaggregate, but they suffer from some of the same difficulties of interpretation as earlier "capping" experiments. Experiments with intact cells cannot, for example, rule out the possibility that 43K associates with AChR only after AChR accumulates into microaggregates.

We used preparations of isolated AChR clusters to avoid some of these difficulties. The several proteins concentrated at isolated AChR clusters cannot be affected by distant regions of the cell surface or by intracellular structures. This preparation has the additional advantage of exposing the entire cytoplasmic face of the cluster membrane to antibodies directed against cytoplasmic epitopes of the AChR, or against receptor-associated proteins on the cytoplasmic side of the membrane.

We have characterized in detail the microaggregation of AChR and related proteins in isolated AChR cluster preparations. Antibody-induced aggregation is specific for proteins present at clusters, as control IgG is ineffective. Microaggregation requires both primary and secondary antibodies, is slowed by cooling to 0°C, and is prevented by fixation. Reorganization of AChR into microaggregates can be followed in individual membrane fragments and is not accompanied by disruption of the lipid bilayer. These results, and the fact that it does not require either cytoplasm or metabolic energy, suggest that microaggregation is analogous to "patching" of antigens in the lymphocyte cell surface (Taylor et al., 1971). A distinction is that microaggregation in our system is driven by antibodies directed

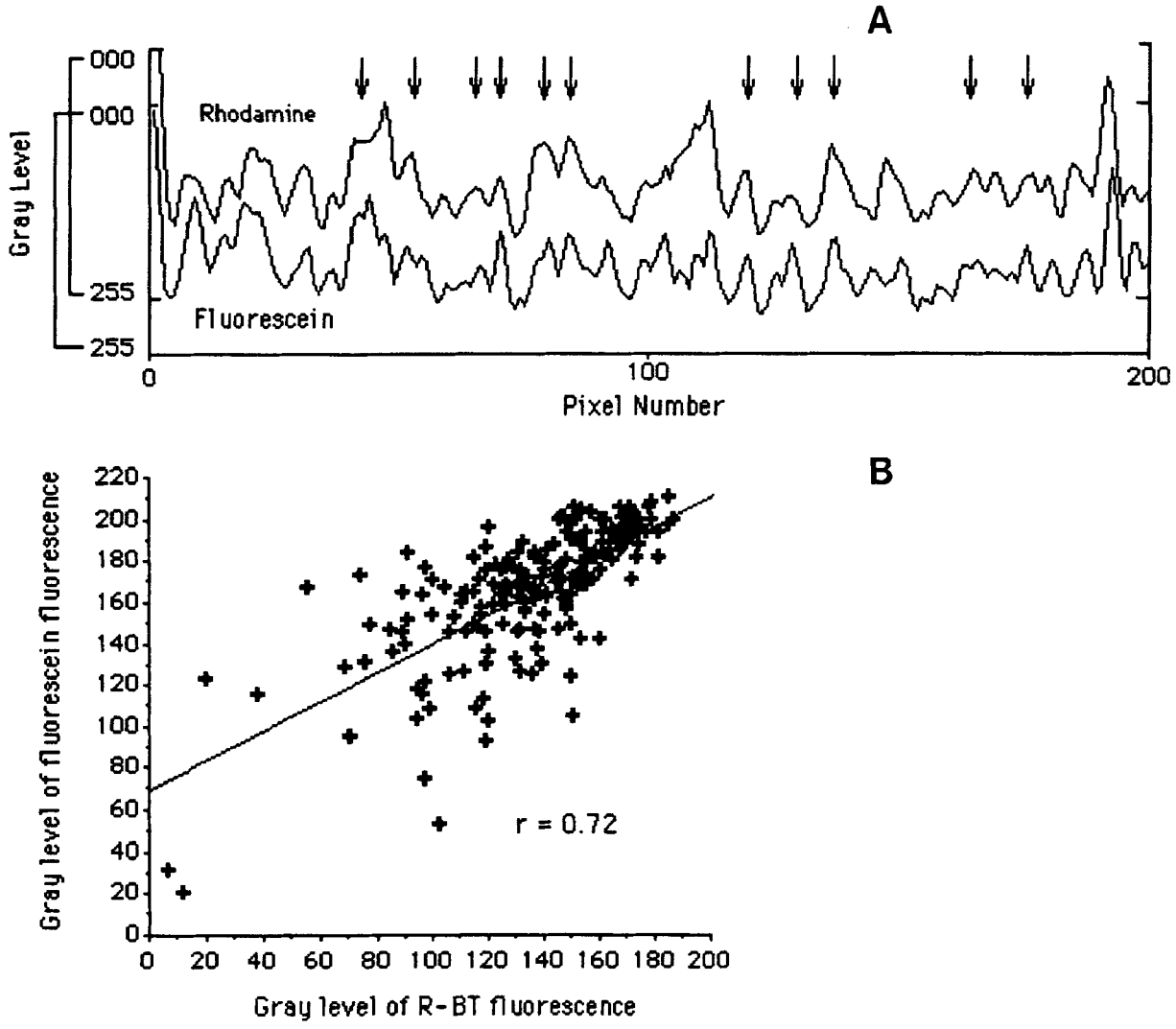

Fig. 8. Correlation of fluorescein and rhodamine fluorescence. Bands three pixels wide were taken at the positions of the black lines in Fig. 6*C,D*. Fluorescent gray levels are plotted as the average of the three-pixel column at each successive position (*A*). The curves for fluorescein (58K) and rhodamine (R-BT) fluorescence are displaced for clarity. The two curves have numerous corresponding regions of high or low fluorescence; several corresponding peaks are indicated by arrows. *B* shows a scattergram of the same data with the gray levels of three-pixel columns from one image plotted against the gray levels of corresponding columns in the other image. The correlation coefficient, 0.72, is highly significant ($P < 0.0001$). Correlation coefficients calculated for bands in the other panels of Fig. 6 were similarly highly significant. Correlation coefficients obtained in the same way, but for two bands that were not from the same region, were not significant ($P > 0.1$).

against epitopes on the cytoplasmic face of the plasma membrane.

We used our microaggregation procedures to assess the relationship between AChR and two proteins, 43K and 58K, which are reported to be closely associated with the receptor. We used antibodies to these proteins, and antibodies to the AChR, to induce microaggregates. We reasoned that, if the AChR and a second protein are closely associated, either directly or indirectly, then the microaggregates of one should contain the other. If, however, the two proteins are not closely associated, or if their association is disrupted by the extraction procedures that precede microaggregation, then they will not appear in the same microaggregates. Although it might be argued that any protein associated with AChR in clusters will coaggregate with receptors, this is not the case. Indeed, in recent experiments, both dystrophin (R.J. Bloch, *unpublished results*) and extracellular matrix proteins (Dymtrenko & Bloch, 1993), which codistribute with AChR in freshly isolated clusters, fail to coaggregate with AChR. Thus, coaggregation is not the result of nonspecific trapping of receptor-associated proteins.

In the case of the 43K receptor-associated protein, our results are consistent with the idea that its association with the AChR is close. Every microaggregate we

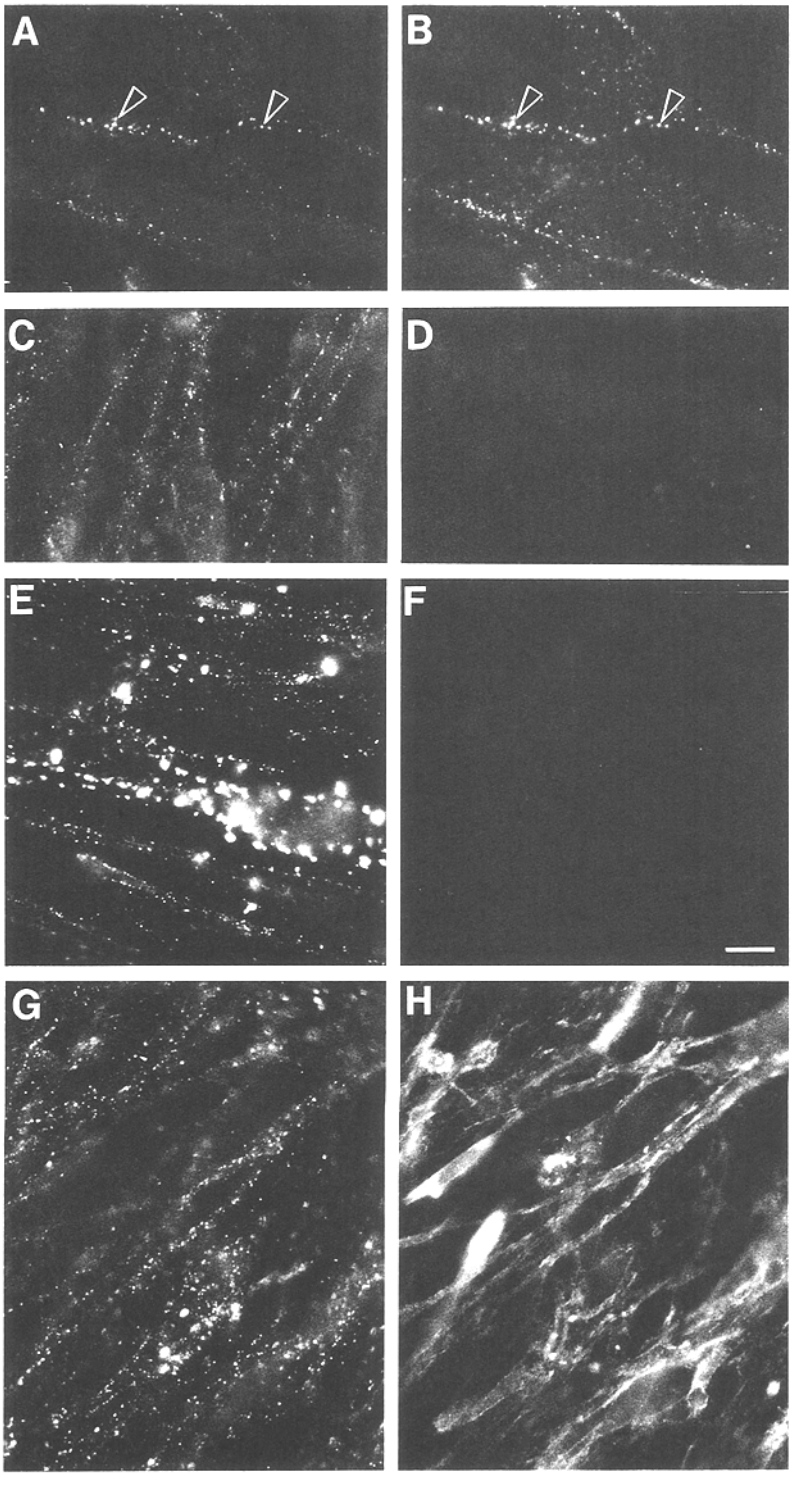

Fig. 9. Microaggregation in intact cells. BC3H-1 cells were labeled with R-BT and incubated with rabbit anti-AChR (*A–D,G,H*) or left unlabeled and incubated with rabbit anti-mouse lymphocyte serum (*E,F*). Cultures were washed and incubated further in sheep anti-rabbit IgG; for the sample in *E* and *F*, this antibody was rhodaminylated. Cultures were fixed, permeabilized and labeled with mouse mab to 43K (*A,B; E,F*), with mab to 58K (*G,H*) or with a control mab (*C,D*), followed by FGAM. *A,C,E* and *G* show rhodamine; *B,D,F* and *H* show fluorescein. (*A,B*) Microaggregates of AChR, labeled with R-BT (*A*, arrowheads) also label with anti-43K mabs and FGAM (*B*, arrowheads). (*C,D*) Microaggregates of AChR (*C*) do not label with a control mouse IgG (*D*). (*E,F*) Microaggregates of other surface antigens, labeled with rhodaminylated antibodies (*E*) do not label with anti-43K and FGAM (*F*). (*G,H*) Microaggregates of AChR, labeled with R-BT (*G*) appear unlabeled by anti-58K mabs and FGAM (*H*). Scale bar = 10 μm.

examined, whether induced by antibodies to AChR or to 43K, contains both proteins. As microaggregation occurs in chymotrypsinized samples, which lack all proteins known to be at the cytoplasmic face of the cluster membrane except 43K, including actin, β-spectrin, 58K and dystrophin (*see* Table 1), these proteins cannot link AChR to 43K. Although other proteins may serve this function, the weight of the biochemical, transfection, and ultrastructural evidence (Sealock, 1982*a*, Burden et al., 1983; Nghiem et al., 1983; Toyoshima & Unwin,

1988; Mitra, McCarthy & Stroud, 1989; Froehner et al., 1990; Phillips et al., 1991), and the results we report here, suggest that 43K and AChR associate directly.

Based on the same microaggregation criteria, we believe that the association of 58K and AChR, like that of 43K and AChR, is also close. Although microaggregates induced by antibodies to the 58K protein are not as clearly visible as those induced by antibodies to the 43K protein, this is probably because we were obliged to use isolated AChR clusters that had been extracted at low ionic strength for these experiments. Unlike chymotrypsin, extraction at low ionic strength fails to remove peripheral membrane proteins (e.g., β-spectrin) that are likely to restrict the movement of AChR in the plane of the membrane. To facilitate analysis of the microaggregates in such clusters, we digitized our images and compared the distribution of 58K and AChR quantitatively. Our results indicate that most of the 58K in cluster membrane is closely associated with AChR, but they do not indicate if this association is direct or indirect.

58K is present in areas of muscle membrane that are not enriched in AChR or 43K (Froehner et al., 1987; Bloch et al., 1991), suggesting that it does not require these proteins for binding to the sarcolemma. Indeed, recent evidence suggests that the 58K protein can bind to dystrophin (Butler et al., 1992) and may be part of a complex linking dystrophin to membrane-bound glycoproteins (Ervasti & Campbell, 1991). Given the ability of 58K to bind to these other proteins, its association with AChR may be indirect. This suggests that the other proteins with which 58K interacts may themselves be closely associated with clustered AChR. Experiments to test this possibility are now in progress.

Considering the close association of 58K and AChR in isolated membrane fragments, it is perhaps surprising that these two proteins did not coaggregate in intact BC3H-1 cells. The explanation for this discrepancy probably lies in the fact that 58K is capable of associating with several different ligands in distinct membrane-skeletal complexes (Ervasti & Campbell, 1991; Butler et al., 1992). If AChR provides only a small fraction of the membrane association sites available to 58K in BC3H-1 cells, it would be difficult to detect their codistribution in microaggregates. By contrast, if few sites other than those associated with AChR are present, as appears to be the case in isolated clusters, coaggregation is easily seen.

Although they are clearly similar to "patching and capping," our microaggregation procedures have several advantages afforded by the use of membrane fragments in substrate-associated material. (i) The participation of intracellular structures is eliminated. (ii) Background signals arising from the cytoplasm are reduced. (iii) The flattened membrane preparations make the aggregation phenomenon more easily studied by fluorescence and ultrastructural techniques. (iv) Direct access by antibodies to proteins lying on the cytoplasmic face of the membrane allows tests of aggregation of an integral membrane protein driven by antibodies to peripheral membrane proteins. Antibody-induced microaggregation in substrate-associated membrane fragments may therefore prove useful in other systems in which biochemical evidence for complex formation is otherwise difficult to obtain.

We thank J. Strong for his expertise in obtaining the data for Figs. 6–8, and W. Resneck, A. O'Neill, and K. Douville for their assistance throughout this work. Our research has been supported by grants from the Muscular Dystrophy Association (to R.J.B., R.S., D.W.P. and S.C.F.) and from the National Institutes of Health (NS17282 to R.J.B.; NS27171 to P.W.L.; NS15513 to D.W.P.; NS15293 to R.S.; NS14871 to S.C.F.).

References

Axelrod, D. 1980. Crosslinkage and visualization of acetylcholine receptors on myotubes with biotinylated alpha-bungarotoxin and fluorescent avidin. *Proc. Natl. Acad. Sci. USA* **77:**4823–4827

Axelrod, D. 1981. Cell-substrate contacts illuminated by total internal reflection fluorescence. *J. Cell Biol.* **89:**141–145

Bloch, R.J. 1979. Dispersal and reformation of acetylcholine receptor clusters of cultured rat myotubes treated with inhibitors of energy metabolism. *J. Cell Biol.* **82:**626–643

Bloch, R.J. 1984. Isolation of acetylcholine receptor clusters in substrate-associated material from cultured rat myotubes using saponin. *J. Cell Biol.* **99:**984–993

Bloch, R.J. 1986. Actin at receptor-rich domains of isolated acetylcholine receptor clusters. *J. Cell Biol.* **102:**1447–1458

Bloch, R.J., Froehner, S.C. 1987. The relationship of the postsynaptic 43K protein to acetylcholine receptors in receptor clusters isolated from cultured rat myotubes. *J. Cell Biol.* **104:**645–654

Bloch, R.J., Geiger, B. 1980. The localization of acetylcholine receptor clusters in areas of cell-substrate contact in cultures of rat myotubes. *Cell* **21:**25–35

Bloch, R.J., Morrow, J.S. 1989. An unusual beta spectrin associated with clustered acetylcholine receptors. *J. Cell Biol.* **108:**481–493

Bloch, R.J., Pumplin, D.W. 1988. Molecular events in synaptogenesis: nerve-muscle adhesion and postsynaptic differentiation. *Am. J. Physiol.* **254:**C345–364

Bloch, R.J., Resneck, W.G., O'Neill, A., Strong, J., Pumplin, D.W. 1991. Cytoplasmic components of acetylcholine receptor clusters of cultured rat myotubes: the 58kD protein. *J. Cell Biol.* **115:**435–446

Burden, S.J., DePalma, R.L., Gottesman, G.S. 1983. Crosslinking of proteins in acetylcholine receptor-rich membranes: Association between the beta-subunit and the 43 kD subsynaptic protein. *Cell* **35:**687–692

Butler, M.H., Douville, K., Murnane, A.A., Kramarcy, N.R., Cohen, J.B., Sealock, R., Froehner, S.C. 1992. Association of the Mr 58,000 postsynaptic protein of electric tissue with *Torpedo* dystrophin and the Mr 87,000 postsynaptic protein. *J. Biol. Chem.* **267:**6213–6218

Cartaud, J., Sobel, A., Rousselet, A., Devanux, P.F., Changeux, J.-P. 1981. Consequences of alkaline treatment for the ultrastructure of the acetylcholine-receptor-rich membranes from *Torpedo marmorata* electric organ. *J. Cell Biol.* **90:**418–426

Changeux, J.-P., Devillers-Thiéry, A., Chemouilli, P. 1984. Acetylcholine receptor: An allosteric protein. *Science* **225:**1335–1345

Cohen, S.A., Pumplin, D.W. 1979. Clusters of intramembrane particles associated with binding sites for α-bungarotoxin in cultured chick myotubes. *J. Cell Biol.* **82:**494–516

Dmytrenko, G.D., Bloch, R.J. 1993. Evidence for transmembrane anchoring of extracellular matrix at acetylcholine receptor clusters. *Exp. Cell Res.* **206:**323–334

Dmytrenko, G.D., Pumplin, D.W., Bloch, R.J. 1992. Dystrophin in a membrane skeletal network: localization and comparison to other proteins. *J. Neurosci.* **13:**547–558

Ervasti, J.M., Campbell, K.P. 1991. Membrane organization of dystrophin-glycoprotein complex. *Cell* **66:**1121–1131

Froehner, S.C. 1981. Identification of exposed and buried determinants of the membrane-bound acetylcholine receptor from *Torpedo californica*. *Biochemistry* **20:**4905–4915

Froehner, S.C. 1984. Peripheral proteins of postsynaptic membranes from *Torpedo* electric organ identified with monoclonal antibodies. *J. Cell Biol.* **99:**88–96

Froehner, S.C. 1991. The submembrane machinery for nicotinic acetylcholine receptor clustering. *J. Cell Biol.* **114:**1–7

Froehner, S.C., Douville, K., Klink, S., Culp, W.J. 1983. Monoclonal antibodies to cytoplasmic domains of the acetylcholine receptor. *J. Biol. Chem.* **258:**7112–7120

Froehner, S.C., Luetje, C.W., Scotland, P.B., Patrick, J. 1990. The postsynaptic 43K protein clusters muscle nicotinic acetylcholine receptors in *Xenopus* oocytes. *Neuron* **5:**403–410

Froehner, S.C., Murnane, A.A., Tobler, M., Peng, H.B., Sealock, R. 1987. A postsynaptic M_r 58,000 (58K) protein concentrated at acetylcholine receptor-rich sites in *Torpedo* electroplaques and skeletal muscle. *J. Cell Biol.* **104:**1633–1646

Heuser, J.E., Salpeter, S.R. 1979. Organization of acetylcholine receptors in quick-frozen, deep-etched, and rotary-replicated *Torpedo* postsynaptic membrane. *J. Cell Biol.* **82:**150–173

Johnson, G.D., Davidson, R.S., McNamee, K.C., Russell, G., Goodwin, D., Holborow, E.J. 1992. Fading of immunofluorescence during microscopy: a study of the phenomenon and its remedy. *J. Immunol. Met.* **55:**231–242

Land, B.R., Podleski, T.R., Salpeter, E.E., Salpeter, M.M. 1977. Acetylcholine receptor distribution on myotubes in culture correlated to acetylcholine sensitivity. *J. Physiol.* **269:**155–176

LaRochelle, W.J., Froehner, S.C. 1986. Determination of the tissue distributions and relative concentrations of the postsynaptic 43KDa protein and the acetylcholine receptor in *Torpedo*. *J. Biol. Chem.* **261:**5270–5274

Lo, M.M.S., Garland, P.B., Lamprecht, J., Barnard, E.A. 1980. Rotational mobility of the membrane-bound acetylcholine receptor of *Torpedo* electric organ measured by phosphorescence depolarisation. *FEBS Lett.* **111:**407–412

Mitra, A.K., McCarthy, M.P., Stroud, R.M. 1989. Three-dimensional structure of the nicotinic acetylcholine receptor and location of the major associated 43-kD cytoskeletal protein, determined at 22 Å by low dose electron microscopy and X-ray diffraction to 12.5 Å. *J. Cell Biol.* **109:**755–774

Neubig, R.R., Krodel, E.K., Boyd, N.D., Cohen, J.B. 1979. Acetylcholine and local anesthetic binding to *Torpedo* nicotinic postsynaptic membranes after removal of nonreceptor peptides. *Proc. Natl. Acad. Sci. USA* **76:**690–694

Nghiem, H.-O., Cartaud, J., Dubreuil, C., Kordeli, C., Buttin, G., Changeux, J.-P. 1983. Production and characterization of a monoclonal antibody directed against the 43,000-dalton υ_1 polypeptide from *Torpedo marmorata* electric organ. *Proc. Natl. Acad. Sci. USA* **80:**6403–6407

Olek, A.J., Pudimat, P.A., Daniels, M.P. 1983. Direct observation of the rapid aggregation of acetylcholine receptors on identified cultured myotubes after exposure to embryonic brain extract. *Cell* **34:**255–264

Pauli, B.U., Weinstein, R.S., Soble, L.W., Alroy, J. 1977. Freeze fracture of monolayer cultures. *J. Cell Biol.* **72:**763–769

Phillips, W.D., Kopta, C., Blount, P., Gardner, P.D., Steinbach, J.H., Merlie, J.P. 1991. ACh receptor rich domains organized in fibroblasts by recombinant 43-kilodalton protein. *Science* **251:**568–570

Porter, S., Froehner, S.C. 1985. Interaction of the 43K protein with components of *Torpedo* postsynaptic membranes. *Biochemistry* **24:**425–432

Pumplin, D.W., Bloch, R.J. 1983. Lipid domains of acetylcholine receptor clusters detected with saponin and filipin. *J. Cell Biol.* **97:**1043–1054

Pumplin, D.W., Bloch, R.J. 1990. Clathrin-coated membrane: a distinct membrane domain in acetylcholine receptor clusters of rat myotubes. *Cell Motil. Cytoskel.* **15:**121–134

Raff, M.C., DePetris, S. 1973. Movement of lymphocyte surface antigens and receptors: the fluid nature of the lymphocyte plasma membrane and its immunological significance. *Fed. Proc.* **32:**48–54

Rousselet, A., Cartaud, J., Changeux, J.-P. 1979. Importances des interactions protéine-protéine dans le maintien de structure des fragments excitables de l'organe éléctrique de *Torpedo marmorata*. *C.R. Seances Acad. Sci.* **289:**461–463

Scher, M.G., Bloch, R.J. 1991. The lipid bilayer of acetylcholine receptor clusters of cultured rat myotubes is organized into morphologically distinct domains. *Exp. Cell Res.* **195:**79–91

Schubert, D., Harris, A.J., Devine, C.E., Heinemann, S. 1974. Characterization of a unique muscle cell line. *J. Cell Biol.* **61:**398–413

Sealock, R. 1982*a*. Cytoplasmic surface structure in postsynaptic membranes from electric tissue visualized by tannic-acid-mediated negative contrasting. *J. Cell Biol.* **92:**514–522

Sealock, R. 1982*b*. Visualization at the mouse neuromuscular junction of a submembrane structure in common with *Torpedo* postsynaptic membranes. *J. Neurosci.* **2:**918–923

Stroud, R.M., Finer-Moore, J. 1985. Acetylcholine receptor structure, function, and evolution. *Annu. Rev. Cell Biol.* **1:**317–351

Taylor, R.B., Duffus, P.H., Raff, M.C., DePetris, S. 1971. Redistribution and pinocytosis of lymphocyte surface immunoglobulin molecules induced by anti-immunoglobulin antibody. *Nature New Biol.* **233:**225–229

Toyoshima, C., Unwin, N. 1988. Ion channel of acetylcholine receptor reconstructed from images of postsynaptic membranes. *Nature* **336:**247–250

Wennogle, L.P., Changeux, J.-P. 1980. Transmembrane orientation of proteins present in acetylcholine receptor-rich membranes from *Torpedo marmorata* studied by selective proteolysis. *Eur. J. Biochem.* **106:**381–393

Yee, A.G., Fischbach, G.D., Karnovsky, M. 1978. Clusters of intramembrane particles in cultured myotubes at sites that are highly sensitive to acetylcholine. *Proc. Natl. Acad. Sci. USA* **75:**3004–3008